GEOLOGIC NOTE

An analysis of horizontal microcracking during catagenesis: Example from the Catskill delta complex

Gary G. Lash and Terry Engelder

ABSTRACT

Horizontal bitumen-filled microcracks are common within clay laminae of the finely laminated organic carbon-rich shale in the lower half of the heavily jointed Upper Devonian Dunkirk Shale, western New York state. Such cracks are not found higher in the Dunkirk Shale, where moderate bioturbation resulted in a relatively porous and permeable microfabric. Horizontal microcracks in a hydrocarbon source rock that carries regional vertical joints indicating a horizontal least principal stress owe their presence to material properties of the fractured shale and the magnitude and orientation of the crack-driving stress during kerogen maturation. Three material properties favored the horizontal initiation of microcracks in the Dunkirk Shale: (1) the abundance of flat kerogen grains oriented parallel to layering; (2) a marked strength anisotropy in large part caused by the laminated nature of the rock; and (3) the tight, strongly oriented planar clay-grain fabric produced by gravitational compaction of flocculated clay at shallow-burial depth. The latter was especially important to sustaining elevated pore pressure, the crack-driving stress, which was generated by the conversion of kerogen to bitumen. Poroelastic deformation of the low-permeability laminated shale pressurized by catagenesis, perhaps enhanced by compaction disequilibrium prior to kerogen conversion, elevated the in-situ horizontal stress in excess of the vertical stress, which remained constant during pore-pressure buildup, thereby favoring the propagation of microcracks in the horizontal plane.

Manuscript received December 20, 2004; provisional acceptance April 4, 2005; revised manuscript received May 23, 2005; final acceptance May 25, 2005.

DOI:10.1306/05250504141

AUTHORS

GARY G. LASH ~ *Department of Geosciences, State University of New York–College at Fredonia, Fredonia, New York 14063; Lash@fredonia.edu*

Gary received his B.S. degree from Kutztown State University and his M.S. degree and his Ph.D. from Lehigh University. Before working in the fractured Upper Devonian shales of the western New York state region of the Appalachian basin, he was involved in stratigraphic and structural investigations of thrusted Cambrian–Ordovician deposits of the central Appalachians.

TERRY ENGELDER ~ *Department of Geosciences, Pennsylvania State University, University Park, Pennsylvania 16802; engelder@geosc.psu.edu*

Terry received his B.S. degree from Pennsylvania State University, where he joined the faculty after tours at Texas A&M University (Ph.D.) and the Lamont-Doherty Geological Observatory (postdoctoral study). After collaborating with him on brittle fracture and earth stress, his former students have moved on to companies including Anadarko, Atlas Western, British Petroleum, Chevron, ExxonMobil, Marathon, Royal Dutch Shell, Schlumberger, Shell U.S.A., and Texaco.

ACKNOWLEDGEMENTS

This article benefited from the reviews of Stephen Cumella and Stephen Laubach. We thank Peter Bush and his staff at the University of Buffalo, South Campus Instrumentation Center, School of Dental Medicine, for help with the electron microscopy. Support also came from Penn State's Seal Evaluation Consortium.

INTRODUCTION

Horizontal microcracks in fine-grained, low-permeability source rocks serve as primary hydrocarbon-migration pathways that, when interconnected, facilitate expulsion into nearby reservoir rocks (Snarsky, 1962; Momper, 1978; du Rouchet, 1981; Talukdar et al., 1987; Özkaya, 1988; Lehner, 1991; Capuano, 1993; Márquez and Mountjoy, 1996). Several investigators maintain that the horizontal propagation of maturation-related microcracks in laminated source rocks is a consequence of a compaction-induced strength anisotropy and/or a concentration of flattened kerogen grains in parallel layers (e.g., Meissner, 1978; Talukdar et al., 1987; Özkaya, 1988; Lehner, 1991; Vernik, 1994). This fracture orientation requires that the cracks opened against the total vertical stress, S_v, which typically, in epeirogenic and continental-margin settings, is the maximum principal stress (e.g., Gaarenstroom et al., 1993; Grauls and Baleix, 1994; Finkbeiner and Zoback, 1998). Because total stress is such a strong governor of crack propagation, it is of interest to investigate conditions under which local or in-situ stresses during hydrocarbon maturation may differ from the most commonly reported basinal stress configuration in which $S_v > S_h$, the total least horizontal stress. Indeed, the few instances where S_v is documented to be the least principal stress have been described from overpressured sedimentary basins (e.g., Ervine and Bell, 1987). It is important to consider whether such in-situ stresses (i.e., $S_v < S_h$) in overpressured source rocks, acting in tandem with material properties, including layer-perpendicular strength anisotropy and kerogen grain shape, can lead to horizontal crack initiation and propagation during catagenesis.

This article documents the growth of horizontal microcracks in the Upper Devonian Dunkirk black shale, one of several Devonian source rocks charging the hydrocarbon system of the Appalachian basin. Our calculations suggest that strength anisotropy, kerogen grain shape, and clay-grain microfabric were instrumental in initiating the horizontal microcracks. Petrographic and SEM observations tie the driving mechanism for microcrack propagation in the organic-rich shale to a buildup of internal pressure that accompanied transformation of kerogen to bitumen. We propose that the pervasive increase in internal pressure caused by catagenesis could have induced a poroelastic response within the Dunkirk source rock during the conversion of kerogen. In its extreme, poroelastic deformation is capable of causing an increase in S_h to the point that $S_h > S_v$, thereby favoring the post-initiation growth of microcracks in the horizontal plane.

DUNKIRK SHALE

The Dunkirk Shale, approximately 17 m (55 ft) of black and grayish-black shale and sparse, thin siltstone beds, is the youngest of the Upper Devonian black shale units of the Catskill delta complex, western New York Appalachian plateau (Figure 1). The shale carries several sets of vertical joints that demonstrate the extent to which the formation was subject to a regional stress state where $S_h < S_v$ (Lash et al., 2004). The presence of these regional joint sets is compelling evidence that horizontal microcrack propagation manifests unusual local or in-situ conditions.

The total organic carbon (TOC) content of the Dunkirk Shale diminishes upsection from a maximum of 4.63 wt.% in exposures along the Lake Erie shoreline near Dunkirk, New York (Figure 1) (Lash et al., 2004). Comparison of (1) the S_2 parameter (second peak in Rock-Eval pyrolysis) with TOC (Figure 2A) and (2) the hydrogen index (HI; mg hydrocarbons/g TOC) with Rock-Eval T_{max} (temperature of maximum release of hydrocarbons of a sample during pyrolysis) (Figure 2B) suggests that organic matter in the Dunkirk Shale is dominantly oil-prone type II kerogen of marine origin. Measured vitrinite reflectance (R_o) values of Dunkirk Shale samples range from 0.55 to 0.73% (average = 0.62%; $n = 6$; Lash et al., 2004), thereby placing this unit close to or within the oil-generating window (Tissot and Welte, 1984; Espitalie, 1986).

The fact that different types of organic matter generate petroleum at different levels of thermal maturity (e.g., Lewan et al., 2002) precludes simple judgments regarding the extent of petroleum generation in a source rock based solely on vitrinite reflectance. We assessed the degree of petroleum generation in the Dunkirk Shale by the calculation of the transformation ratio, TR, using HI values according to the following expression:

$$TR = \frac{HI_o - HI_m}{HI_m} \quad (1)$$

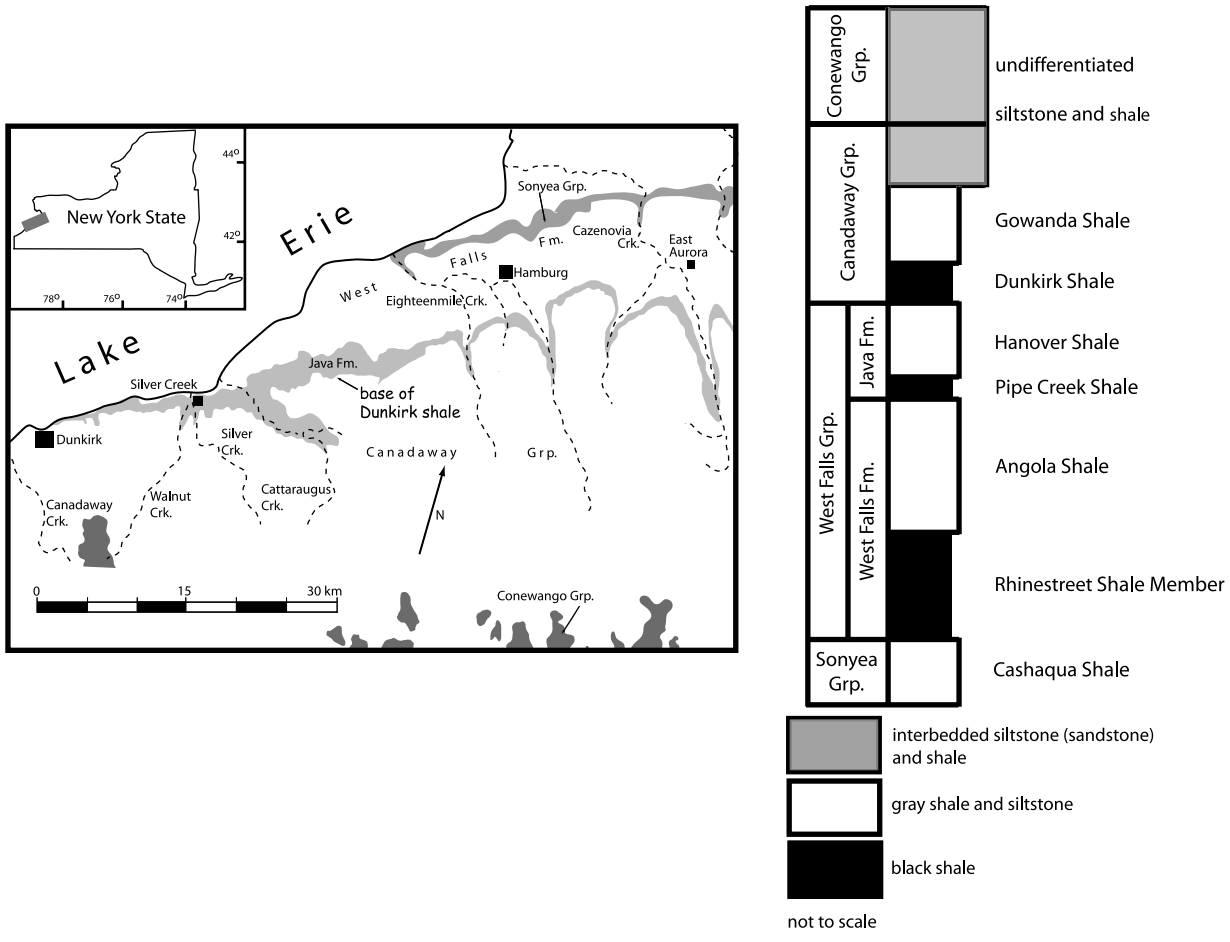

Figure 1. Location map and generalized stratigraphic column of the Upper Devonian sequence of western New York.

in which HI_o and HI_m are hydrogen index values for thermally immature and mature source rocks, respectively. The transformation ratio expressed in this way ranges from 0 for thermally immature rocks to 1.0 for complete transformation of kerogen to hydrocarbons. For HI_o, we used the HI value (399 mg hydrocarbons/g TOC) of that sample defined by an R_o of 0.55%. A shale sample collected about 1.5 m (4.9 ft) above the aforementioned sample has an HI of 416 mg hydrocarbons/g TOC, a value that might be closer to the prematuration HI. The HI of the most thermally mature Dunkirk Shale sample (R_o = 0.73%), 355 mg hydrocarbons/g TOC, was used for HI_m. The calculated TR of the Dunkirk Shale then falls in the range of 0.11–0.13, a bit above that value generally accepted to mark the onset of petroleum generation (0.1; Jarvie and Lundell, 2001). However, inasmuch as our HI_o value was obtained from a sample that may already have generated hydrocarbons (R_o = 0.55%), we view our calculated TR as a minimum estimate.

SHALE MICROFABRIC AND HORIZONTAL MICROCRACKS

Microscopic (thin-section and SEM) analysis of the Dunkirk Shale was conducted to assess those microfabric features, including microcracks, that could have sustained primary migration through the organic-rich shale. Samples were recovered from deeper than 5 cm (2 in.) into exposures to avoid collection from the weathered, fissile veneer that covers most outcrops. Standard petrographic thin sections cut perpendicular to bedding were prepared from each shale sample. The abundance of silt (quartz and feldspar) was quantified by visual estimate using standard comparison charts (Flügel, 1982). Samples were prepared for SEM following the methods outlined by O'Brien and Slatt (1990). Each shale sample was mounted on double-sided adhesive carbon tape such that the viewing direction was normal to bedding. Samples were coated with 20 nm of evaporated carbon to render the surface conductive

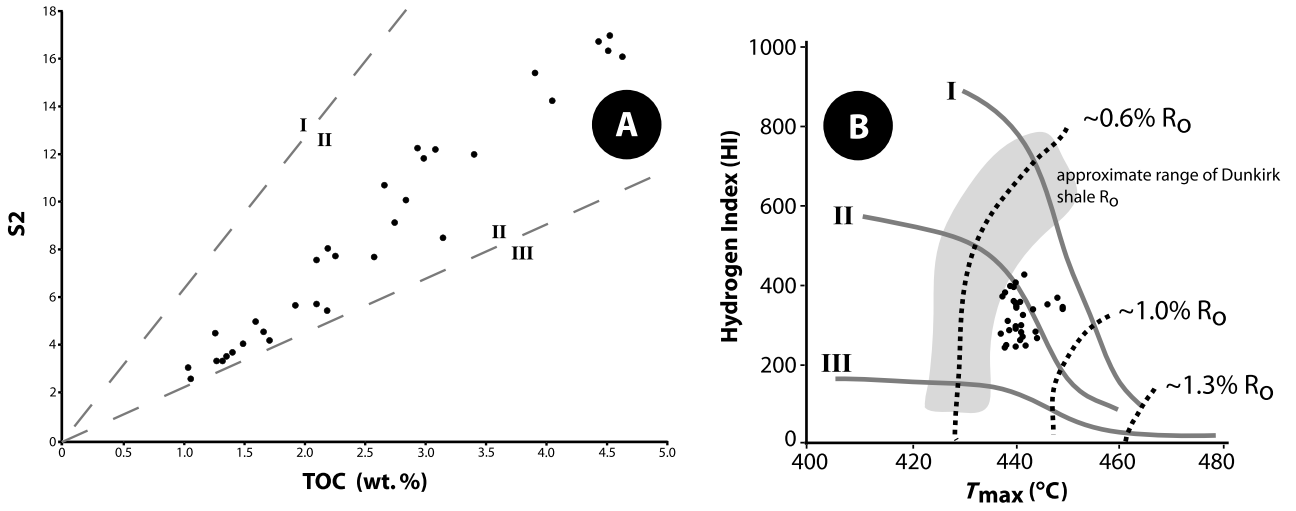

Figure 2. Plots of (A) Rock-Eval S_2 versus TOC% showing fields for types I, II, and III kerogen (modified from Langford and Blanc-Valleron, 1990) and (B) Rock-Eval hydrogen index (HI) versus Rock-Eval T_{max} for the Dunkirk Shale data (n = 32).

and analyzed on a Hitachi S-4000 Field Emission SEM operating at 30 keV. Digital secondary electron images were collected with a 4PI digital imaging system. Both secondary and backscattered modes were used in this work, and elemental analysis was carried out by use of an energy-dispersive x-ray unit.

Petrographic examination of a suite of samples collected from the base to the top of the Dunkirk Shale reveals that the unit is dominated by two black shale types: finely laminated black shale and silty, moderately bioturbated black shale. The former, which dominates approximately the lower third to half of the Dunkirk Shale, is characterized by generally continuous thin to thick (>0.1-mm; >0.004-in.) quartz silt laminae (about 40–50% of the sample) that alternate with dark, silt-poor (<20%) carbonaceous clay layers (Figure 3A). Scanning electron microscopy shows the organic-rich clay layers to be defined by a tight, strongly oriented planar arrangement of clay grains and flattened organic particles (Figure 3B), locally disrupted by angular silt grains and pyrite framboids (Figure 3C). Silt laminae show a much more open or porous microfabric. Angular quartz silt grains appear to have resisted compaction stress, thereby shielding or preserving abnormally large (>10-μm) pores, some of which are filled with diagenetic calcite (Figure 3D), as well as a random clay fabric in interstices of silt grains (Figure 3E). Some silt laminae contain irregular masses of bitumen, suggesting migration from adjacent organic-rich clay laminae (Figure 3F). Finely laminated black shale deposits are the most organic rich of the Dunkirk Shale (≈2.5 < TOC < 4.6%); however, visual examination reveals that organic matter is concentrated in clay laminae where TOC may exceed 50% by volume (Figure 3A). Anoxic bottom conditions during accumulation of finely laminated black shale probably precluded bioturbation of the sediment, thereby preserving the bulk of its organic carbon (Demaison and Moore, 1980) and its finely laminated depositional fabric.

The moderately bioturbated black shale, most common to the upper part of the Dunkirk Shale, lacks the laminated fabric of finely laminated black shale; instead, angular silt grains (>60%) are distributed throughout the organic-rich clay matrix (Figure 4A). Disrupted silt laminae and/or flattened silt-filled burrows (Figure 4A, B) indicate that the sediment was partially reworked by burrowing organisms. Scanning electron microscopic observations of moderately bioturbated black shale samples show a moderately planar to open clay-grain microfabric; angular quartz silt grains are more or less evenly distributed throughout the clay matrix (Figure 4C). The open microfabric of moderately bioturbated black shale deposits likely reflects the homogenizing and disruptive effect of bioturbation and the shielding effect of rigid silt grains during gravitational compaction (Figure 4D) (e.g., Krushin, 1997; Dewhurst et al., 1998).

Horizontal microcracks generally occur as isolated structures, although locally they comprise dense networks, within finely laminated black shale clay laminae (Figure 5A–C). Microcracks commonly are more than 80 μm long (some >250 μm) and have apertures

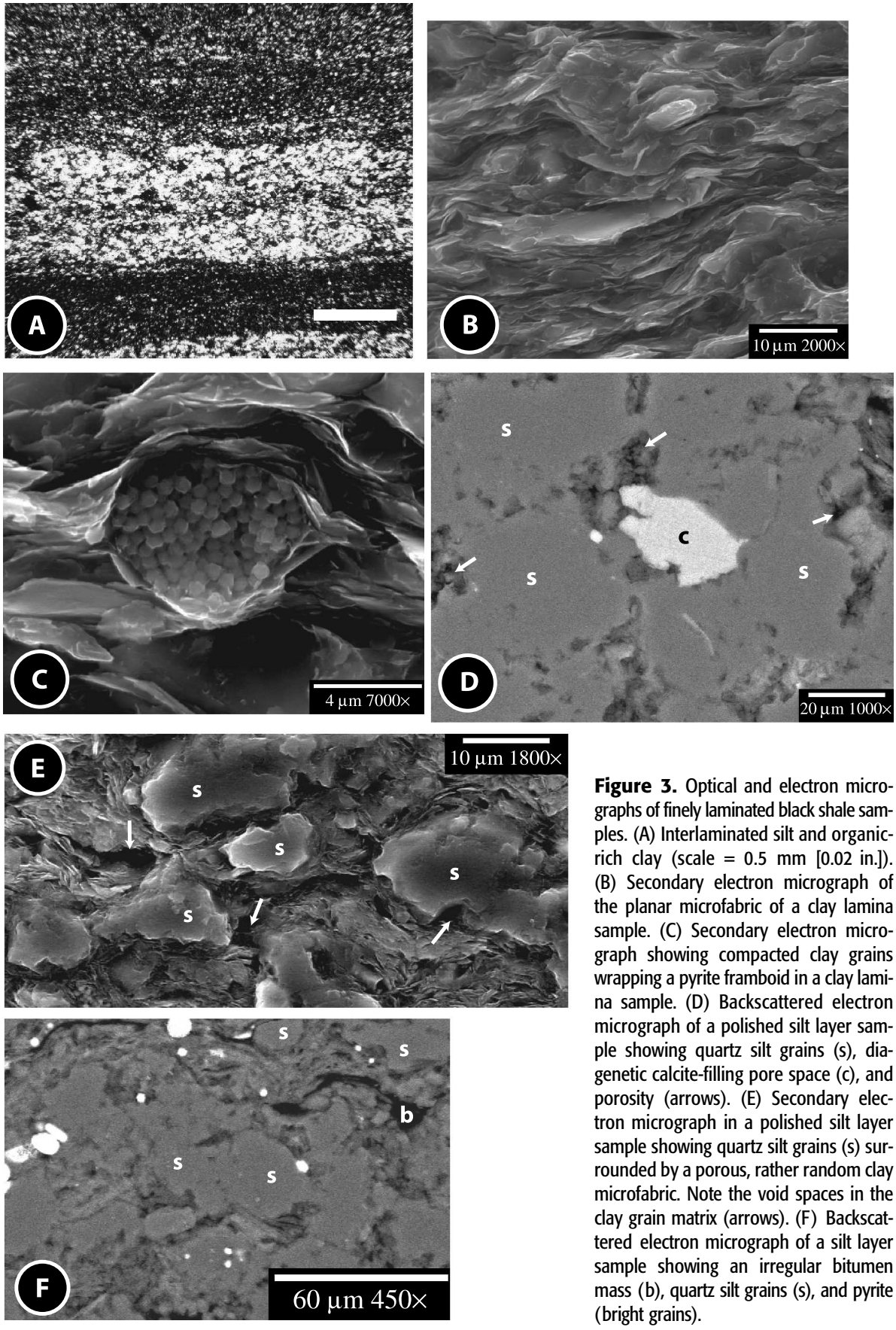

Figure 3. Optical and electron micrographs of finely laminated black shale samples. (A) Interlaminated silt and organic-rich clay (scale = 0.5 mm [0.02 in.]). (B) Secondary electron micrograph of the planar microfabric of a clay lamina sample. (C) Secondary electron micrograph showing compacted clay grains wrapping a pyrite framboid in a clay lamina sample. (D) Backscattered electron micrograph of a polished silt layer sample showing quartz silt grains (s), diagenetic calcite-filling pore space (c), and porosity (arrows). (E) Secondary electron micrograph in a polished silt layer sample showing quartz silt grains (s) surrounded by a porous, rather random clay microfabric. Note the void spaces in the clay grain matrix (arrows). (F) Backscattered electron micrograph of a silt layer sample showing an irregular bitumen mass (b), quartz silt grains (s), and pyrite (bright grains).

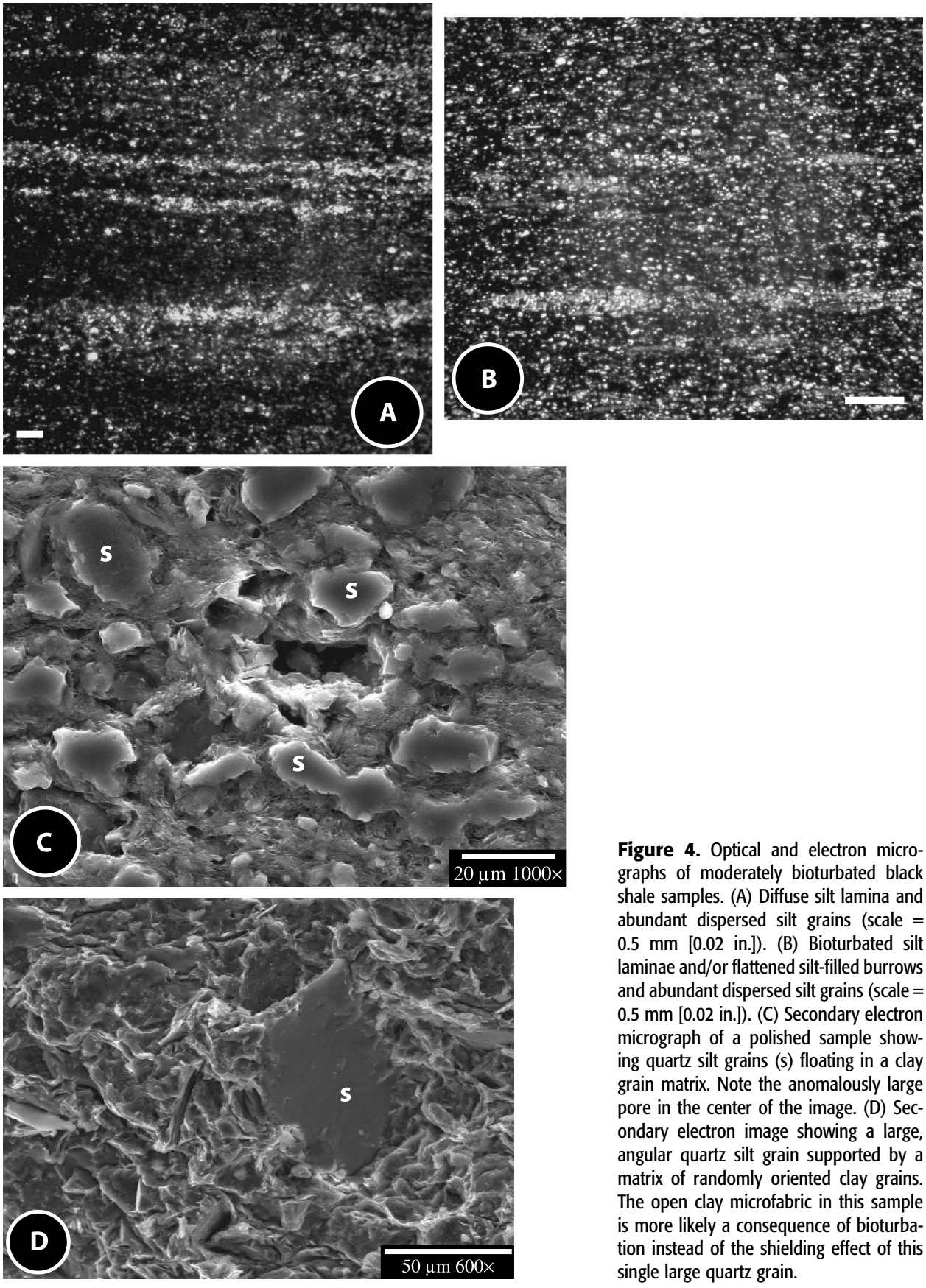

Figure 4. Optical and electron micrographs of moderately bioturbated black shale samples. (A) Diffuse silt lamina and abundant dispersed silt grains (scale = 0.5 mm [0.02 in.]). (B) Bioturbated silt laminae and/or flattened silt-filled burrows and abundant dispersed silt grains (scale = 0.5 mm [0.02 in.]). (C) Secondary electron micrograph of a polished sample showing quartz silt grains (s) floating in a clay grain matrix. Note the anomalously large pore in the center of the image. (D) Secondary electron image showing a large, angular quartz silt grain supported by a matrix of randomly oriented clay grains. The open clay microfabric in this sample is more likely a consequence of bioturbation instead of the shielding effect of this single large quartz grain.

on the order of 3–10 μm (Figure 5A, B). Most cracks are filled with bitumen (Figure 5B, D), as indicated by higher-than-background levels of molybdenum, lead, and sulfur (e.g., Lomando, 1992; Kattai, 1994); we observed that fewer than 20% of the cracks are open or contain nothing more than pyrite crystallites (Figure 5B). Some microcracks contain inclusions of wall rock (clay-grain fragments) within bitumen (Figure 5E). The presence of bitumen as the only crack-filling material indicates that microcracking occurred during, and as a consequence of, the decomposition of kerogen to bitumen (e.g., Comer and Hinch, 1987).

The microcracks are mode I cracks (opening perpendicular to the crack surfaces with a shear stress of zero) as indicated by the close match of grain shapes across apertures (Figure 5E), the lack of evidence for shear offset along cracks, and observations of grains being wedged apart by propagating cracks (Figure 5F, G). Microcracks are approximately parallel to layering and likely propagated along paths controlled by the planar clay-grain microfabric of the host sediment. Finally, microcracking was concentrated along the edges of grains (Figure 5G); rarely did cracks propagate through grains other than clay-grain books. These observations, then, are consistent with previous conclusions that maturation-related microcracks are commonly horizontal (e.g., Meissner, 1978; Talukdar et al., 1987; Littke et al., 1988; Capuano, 1993; Vernik, 1994; Pitman et al., 2001).

CONDITIONS LEADING TO HORIZONTAL MICROCRACKING WITHIN THE DUNKIRK SHALE

Horizontal microcracks formed preferentially in finely laminated black shale clay laminae in the lower interval of the Dunkirk Shale, where they propagated from within flattened kerogen grains or from along kerogen-mineral interfaces (Figure 6). The abundant, relatively impermeable clay laminae most likely sustained internal pressure at a level high enough to drive microcracks during the conversion of kerogen to hydrocarbons. The relatively permeable microfabric of moderately bioturbated black shale deposits higher in the Dunkirk Shale, however, enabled these sediments to more readily expel fluids released by catagenesis. Indeed, previous considerations of microcracking in source rocks suggest that horizontal microcracking requires the buildup and maintenance of pore pressure, P_p, under undrained conditions (e.g., Özkaya, 1988a; Lehner, 1991).

The general equation governing crack propagation according to linear elastic fracture mechanics specifies that the crack-tip stress intensity, K_I, must equal or exceed the strength of the rock according to

$$K_I = \Delta\sigma Y\sqrt{\pi c} \geq K_{Ic} \quad (2)$$

where K_{Ic} is the fracture toughness, c is the crack half-length, Y is the shape factor, and $\Delta\sigma$ is the crack-driving stress. The latter parameter reflects the superposition of P_p on the least compressive total principal stress (i.e., σ_3, which may be either S_v or S_h, depending on local conditions) in a basin so that $\Delta\sigma = P_p - S_v\ (= \sigma_3)$ for horizontal microcrack propagation. Equilibrium crack propagation, then, is a balance among the shape and length of the crack, the strength of the rock, and the crack-driving stress. These parameters can be grouped into two general classes depending on whether they are a manifestation of some material property (i.e., K_{Ic}, Y, and c) or they arise from boundary conditions (i.e., $\Delta\sigma$). Crack-driving stress, which was achieved through a maturation-related increase in P_p, and material properties have different functions in the development and growth of horizontal microcracks in the Dunkirk black shale and thus will be treated separately.

The Role of Material Properties: Horizontal Initiation as a Consequence of Kerogen Grain Shape and Strength Anisotropy

Rock material properties, including layer-perpendicular strength anisotropy and the shape of initiation flaws for microcrack propagation, evolve during consolidation. Soon after deposition, flocculated organic-rich clay laminae of unbioturbated, finely laminated black shale deposits of the Dunkirk Shale underwent rapid mechanical compaction into a tight, mechanically stable planar microfabric (e.g., Lash and Blood, 2004). Interlaminated silt-rich layers, however, did not experience the same degree of compaction strain, a consequence of the shielding effect of the rigid silt grains that preserved a more random clay fabric and anomalously large pores (e.g., Krushin, 1997; Katsube and Williamson, 1998; Dewhurst et al., 1998). Further burial carried the Dunkirk Shale to the top of the oil window by the end of the Carboniferous (Lash et al., 2004), by which time the permeability of the laminated sequence had

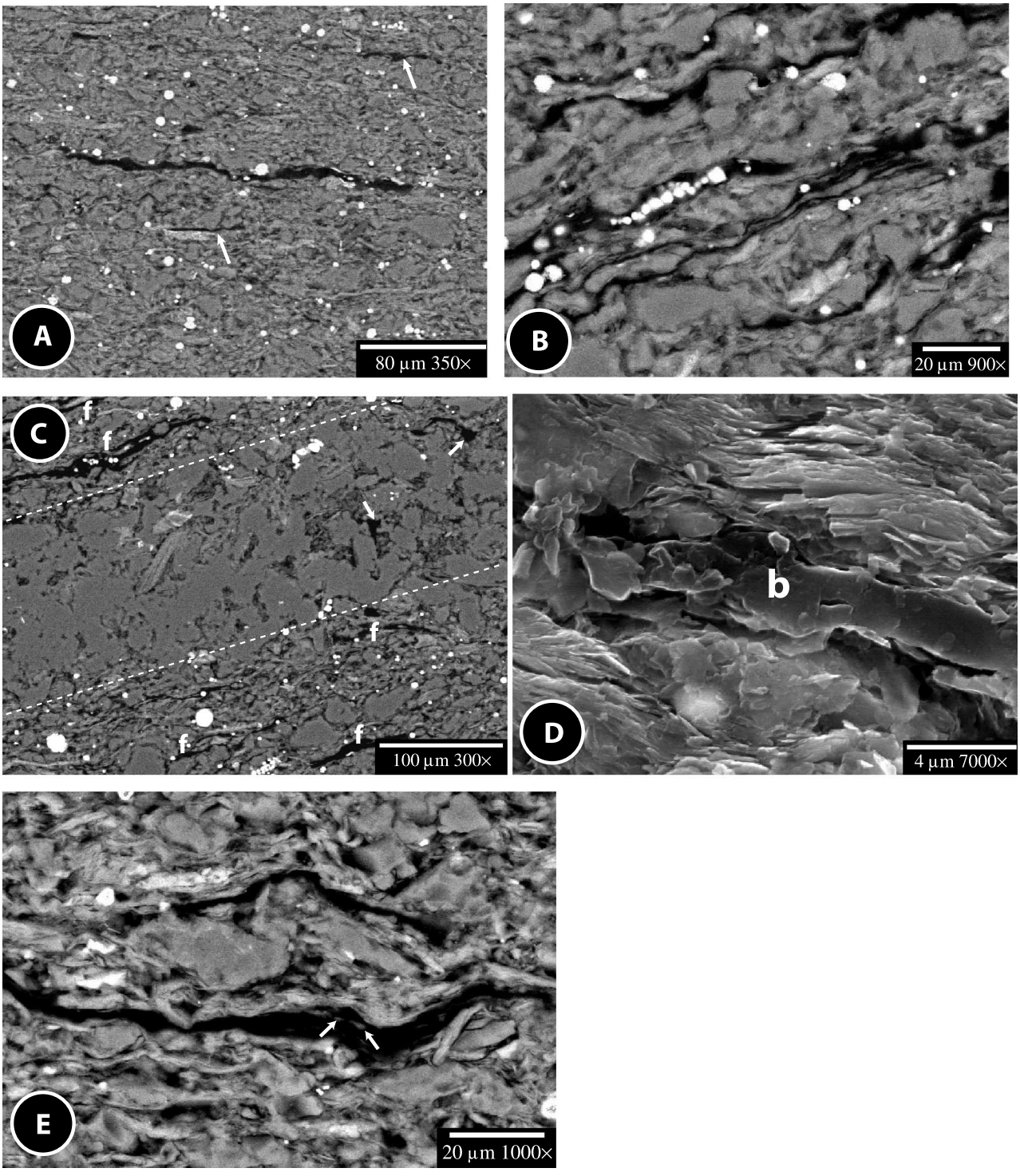

Figure 5. Scanning electron images of horizontal microcracks in finely laminated black shale samples of the Dunkirk Shale. (A) Backscattered electron micrograph of a polished sample showing an isolated large microcrack and two small ones (arrows). (B) Backscattered electron micrograph of a polished finely laminated black shale sample showing a network of closely spaced microcracks. Most cracks are filled with bitumen; some contain pyrite crystallites (bright objects). (C) Backscattered electron image of a polished sample showing a silt lamina (defined by dashed lines), microcracks (f) preferentially developed in clay-rich laminae adjacent to the silt layer, and irregular bitumen masses in the silt layer (arrows). (D) Secondary electron image showing bitumen (b) filling a microcrack. (E) Backscattered electron image of a polished sample showing a bitumen-filled microcrack containing inclusions of the clay grain matrix (arrows). (F) Backscattered electron image of a polished sample showing the tip of a microcrack propagating along clay (c) and quartz (q) grain edges. (G) Large (a) and small (b) microcracks that appear to have propagated along the edges of grains.

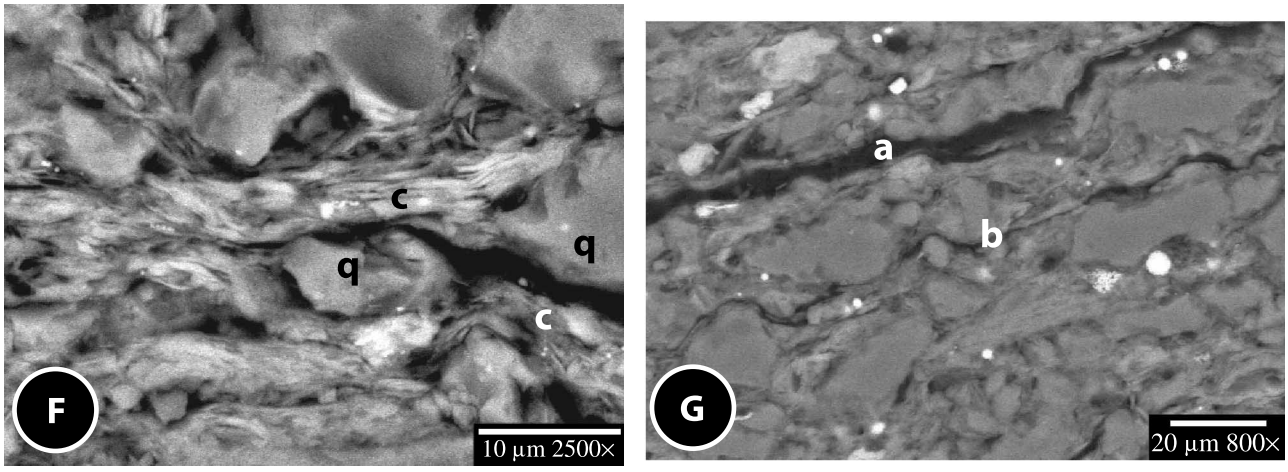

Figure 5. Continued.

been reduced to such a point that pore fluid prevented further compaction and the rock became uniformly overpressured (e.g., Swarbrick et al., 2002).

The geometric form or aspect ratio, ξ, of the organic particles concentrated in specific layers of laminated source rocks may influence the initiation of horizontal microcracks under a basinal stress system in which $S_h = \sigma_3$ favors the propagation of vertical joints. Initiation of horizontal microcracks in a low-permeability oil source rock as a function of kerogen grain shape and strength anisotropy under constant pressure is represented by Özkaya's (1988) equation:

$$\Delta P_p > \frac{S_v(2 - R) + T}{2\xi - 1} \tag{3}$$

where ΔP_p is the increment of internal pressure (the crack-driving stress, $\Delta\sigma$) necessary to initiate a horizontal crack during transformation of a kerogen grain of aspect ratio ξ to oil; R is the stress ratio for uniaxial stress conditions $\left(\frac{S_h}{S_v}\right)$; and T is the tensile strength of the rock measured perpendicular to layering. Although by no means a rigorous expression of crack-tip stress intensity, equation 3 illustrates that $\Delta\sigma$ for crack initiation is inversely proportional to ξ, i.e., the greater the aspect ratio of the kerogen flake, the lower the internal pressure increment necessary to initiate horizontal microcracks.

Preferential horizontal microcracking of finely laminated black shale clay laminae of the Dunkirk Shale probably was facilitated by the strongly oriented clay-grain microfabric and the resultant low K_{IC} normal to bedding of these deposits (e.g., Schmidt, 1977; Costin, 1981; Lehner, 1991; Vernik, 1994). Indeed, Schmidt (1977) demonstrated that the tensile strength of oil shale normal to layering may be as little as one quarter that measured parallel to bedding. For simplicity, we use Schmidt's empirically determined 3-MPa value for T perpendicular to layering in organic-rich shale.

Organic-rich clay layers of the finely laminated black shale deposits contain abundant, rather densely packed, variably flattened kerogen particles, most of which are oriented subparallel to layering (Figure 7A). Much of the organic matter appears as medium to light brown, generally moderately to highly elongate amorphous particles. Lesser dark brown and black vitrinite flakes and dark-orange tasmanite alganite grains are also observed (Figure 7B). Analysis of more than 200 of the most readily measured organic particles in clay laminae samples collected from the lower part of the Dunkirk Shale reveals a wide range of ξ, from about 1 to more than 30 (Figure 8), that probably reflects the original (precompaction) shape of the kerogen, the degree of compaction or flattening sustained by the organic particles, and the local influence of the shielding effect of rigid quartz grains during gravitational compaction. Keeping in mind that we can describe ξ only in two dimensions, our studied population of kerogen grains is defined by three peaks in the distribution of ξ: approximately 2.5, 15, and 29 (Figure 8).

The Breckels and van Eekelen (1982) relationship for S_h as a function of S_v based on well data from the United States Gulf Coast may yield a reasonable estimate of total stress conditions in the Dunkirk Shale at maximum burial:

$$S_h = 0.197z^{1.145} + 0.46(P_p - P_{hyd}) \tag{4}$$

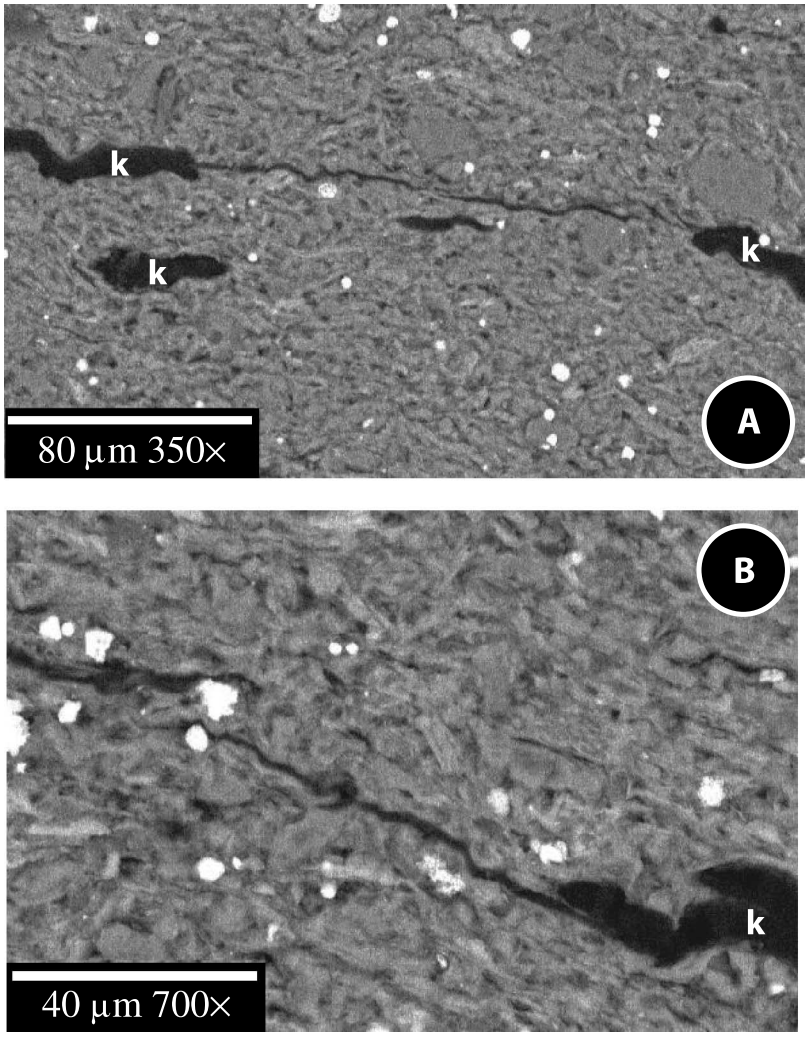

Figure 6. Backscattered electron images of polished finely laminated black shale samples showing microcracks that appear to have originated within (or along the edges of) kerogen (k) particles.

in which z is the depth in feet and S_h, P_p, and P_{hyd} (pore-fluid pressure at hydrostatic conditions) are in pounds per square inch absolute. The estimated S_v of the Dunkirk Shale at its modeled maximum depth of burial of 2.3 km (1.4 mi) (Lash et al., 2004), based on a lithostatic gradient of 22.62 MPa km^{-1} (Harrold et al., 1999), is 52 MPa; P_{hyd} at that depth, using a hydrostatic gradient of 10.18 MPa km^{-1}, is 23.4 MPa. Assuming that the burial history of the Dunkirk Shale is analogous to the subsidence history of the Gulf Coast, and that kerogen in the Dunkirk Shale started to convert to bitumen at hydrostatic conditions, the uniaxial stress ratio $R = \frac{S_h}{S_v} = 0.72$. However, because stress measurements presented by Breckels and van Eekelen (1982) come largely from reservoir rocks (i.e., sandstones), $R = 0.72$ may be a more appropriate measurement of stress in moderately bioturbated black shale deposits instead of finely laminated black shale.

The state of stress in the finely laminated black shale deposits in the lower half of the Dunkirk Shale may be better understood as a product of uniaxial consolidation, where S_h was generated by overburden through the coefficient of earth stress at rest, K_0. For unlithified sediment

$$S_h = K_0(S_v - P_p) + P_p \tag{5}$$

with $S_v = g\rho_{ob}z$, where z = depth and ρ_{ob} = integrated density of overburden (Lambe and Whitman, 1969), and g = gravitational constant. The uniaxial stress ratio for consolidated sediment in an epeiric basin may be calculated as

$$R = \frac{S_h}{S_v} = \frac{K_0(S_v - P_p) + P_p}{S_v} \tag{6}$$

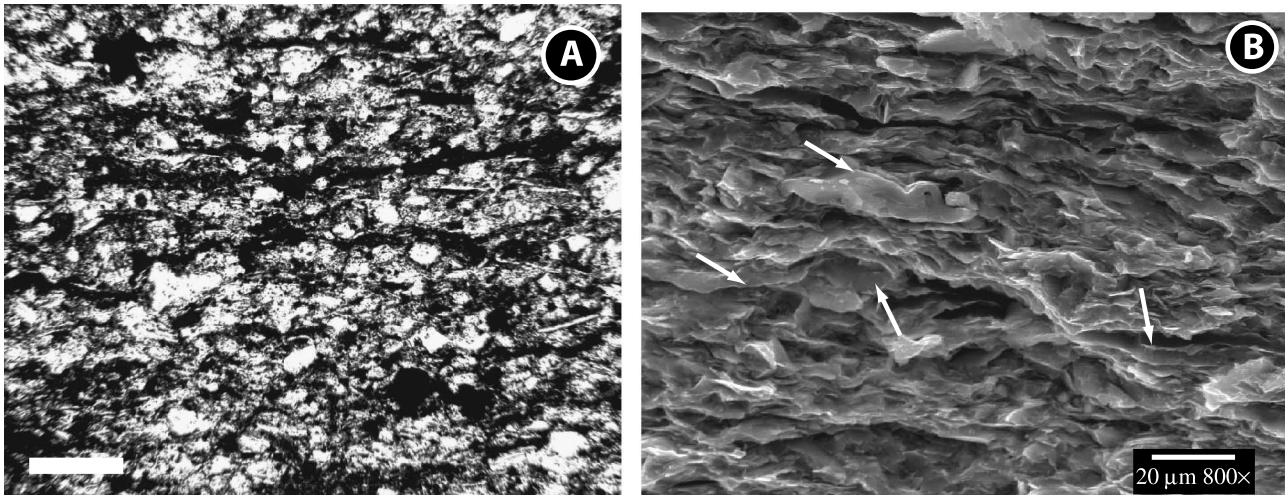

Figure 7. Photomicrographs of organic particles in finely laminated black shale samples. (A) Flattened kerogen grains. Note that the kerogen particles have been compressed to conform to the shape of inorganic grains (scale = 0.1 mm [0.004 in.]). (B) Secondary electron image of a clay lamina sample. Note planar microfabric and flattened organic particles, mostly flattened tasmanite cysts (white arrows).

If K_0 remains constant with increasing depth, R will also remain unchanged as long as the sediment is drained. Consolidation tests simulating drained burial (i.e., $S_v - P_p > 35$ MPa) reveal that K_0 (= 0.62) for silty clay is a constant to $z > 2$ km (1.2 mi); however, K_0 increases slightly for fine sand (K_0 = 0.44–0.53) buried to 2 km (1.2 mi) (Karig and Hou, 1992; Karig and Morgan, 1994). Thus, assuming that the compacting finely laminated black shale deposits of the Dunkirk Shale had a K_0 of silty clay, $R = 0.79$ as long as drained conditions prevailed. The uniaxial stress ratio for sandier parts of the Catskill delta may have increased with increasing burial depth from 0.70 to 0.74 for the same drained conditions and is more consistent with the Breckels and van Eekelen's (1982) data from Gulf of Mexico reservoir rocks.

We assume that prior to catagenesis, P_p in kerogen particles completely supported overburden stress, i.e., $P_p = S_v$. Conversion of kerogen to oil (via an intermediate bitumen phase; e.g., Lewan, 1987) produced an increment of P_p (ΔP_p, the crack-driving stress, $\Delta\sigma$) that pressurized the rock matrix around the kerogen particle. Solving for ΔP_p in equation 3, we find that the minimum ΔP_p required to induce horizontal microcracks

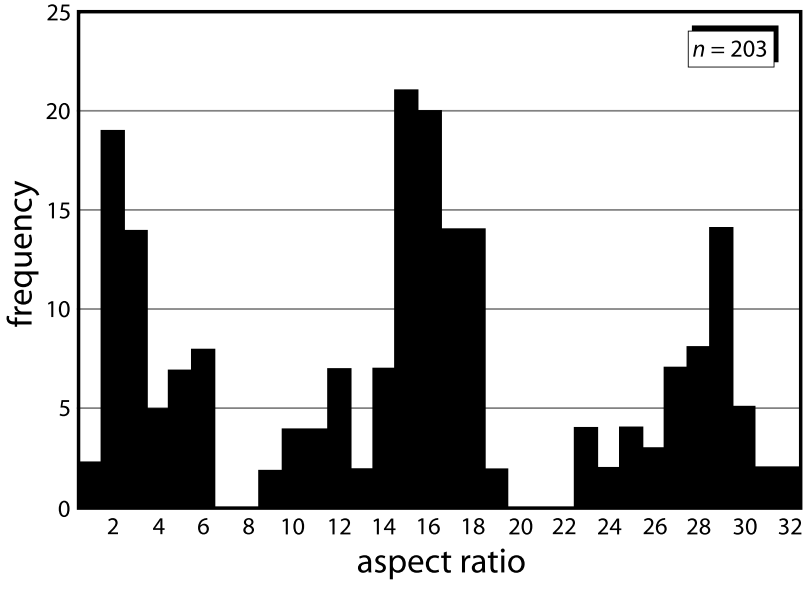

Figure 8. Frequency plot of aspect ratios (ξ) of measured kerogen particles in clay layers of finely laminated black shale deposits.

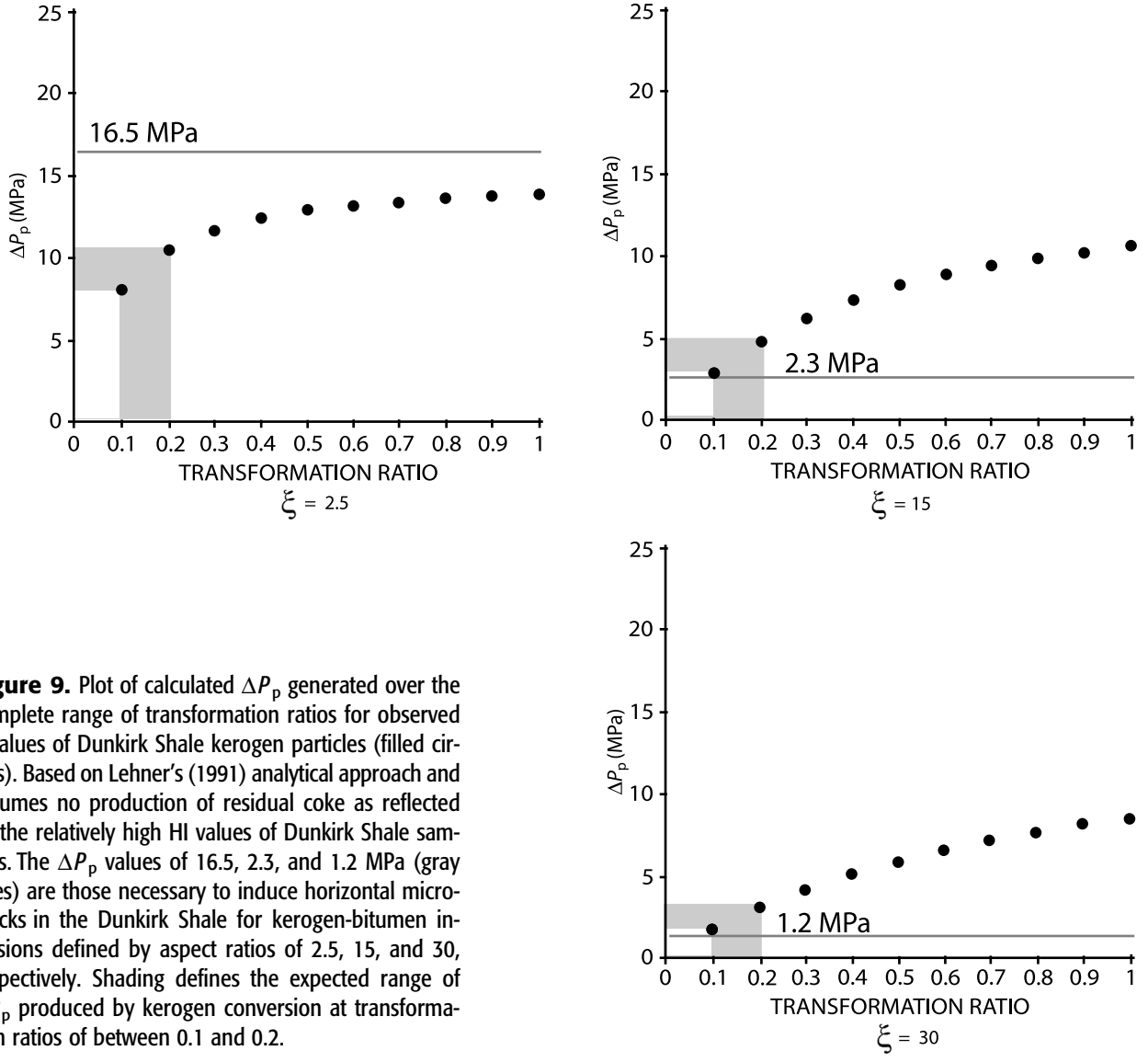

Figure 9. Plot of calculated ΔP_p generated over the complete range of transformation ratios for observed ξ values of Dunkirk Shale kerogen particles (filled circles). Based on Lehner's (1991) analytical approach and assumes no production of residual coke as reflected by the relatively high HI values of Dunkirk Shale samples. The ΔP_p values of 16.5, 2.3, and 1.2 MPa (gray lines) are those necessary to induce horizontal microcracks in the Dunkirk Shale for kerogen-bitumen inclusions defined by aspect ratios of 2.5, 15, and 30, respectively. Shading defines the expected range of ΔP_p produced by kerogen conversion at transformation ratios of between 0.1 and 0.2.

in finely laminated black shale clay laminae of the Dunkirk Shale during conversion of the flattest kerogen grains ($\xi = 29$) to oil is only 1.2 MPa. However, the ΔP_p necessary to initiate horizontal microcracks from the more equidimensional kerogen particles ($\xi = 2.5$) is 16.5 MPa.

The ΔP_p generated by the conversion of a kerogen grain of a specific aspect ratio, ξ, at a given transformation ratio, TR, can be calculated using Özkaya's (1988) value for the compressibility of oil (10^{-2} MPa^{-1}) and Lehner's (1991) compressibility values for kerogen and residual coke and his equations 14, 15, and 19. Comparison of ΔP_p produced by conversion of kerogen grains of aspect ratios of 2.5, 15, and 30 to petroleum at the estimated TR of the Dunkirk Shale (0.1–0.2) with the ΔP_p required to initiate microcracks from kerogen grains of these aspect ratios suggests that (1) horizontal microcracks observed in the Dunkirk Shale were generated from the flattest kerogen grains, and (2) microcracks would not have been initiated from the more equidimensional ($\xi = 2.5$) grains despite the relatively high ΔP_p (8–11 MPa) produced by transformation of these organic particles (Figure 9). Indeed, our calculations suggest that for the inferred burial depth and stress conditions of the Dunkirk Shale outlined above, kerogen particles with $\xi < 4.5$ could not have originated microcracks unless TR ≥ 0.2 (Figure 10).

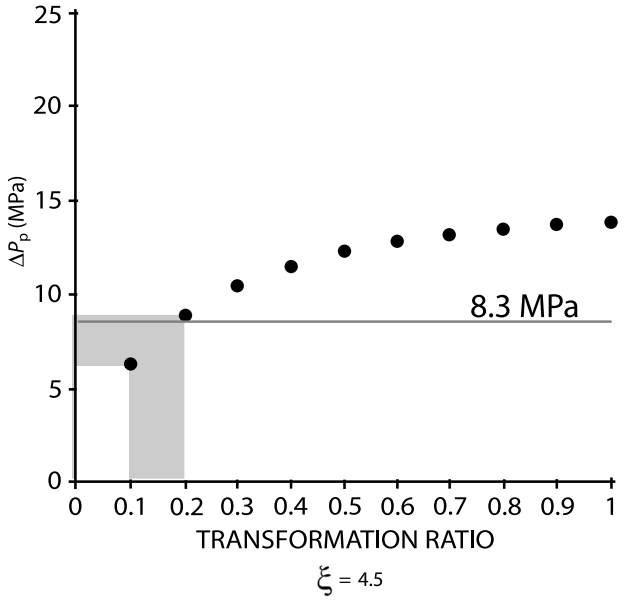

Figure 10. Plot of calculated ΔP_p generated over the complete range of transformation ratios for conversion of kerogen particles of ξ = 4.5 to oil (filled circles). The ΔP_p value of 8.3 MPa is that value necessary to induce horizontal microcracks from kerogen particles defined by an aspect ratio of 4.5. Shading defines the expected range of ΔP_p produced by the conversion of kerogen at transformation ratios of between 0.1 and 0.2.

The Role of Stress: Horizontal Propagation as a Consequence of Poroelastic Deformation

Kerogen particle shape and strength anisotropy of the finely laminated black shale deposits of the Dunkirk Shale favored the initiation of horizontal microcracks. Following this, though, the direction of crack growth would have been controlled by the state of stress, which, for the early subsidence history of an epeiric basin affected by minimal tectonic stress, is defined as $S_h < S_v$ and at odds with the propagation of microcracks in the horizontal plane. Below, we postulate that it was the local state of stress in the finely laminated black shale deposits that most influenced the orientation of crack growth (e.g., Lawn, 1993).

Abnormal pore pressure in a subsiding basin is first generated by compaction disequilibrium caused by the inability of pore fluid to drain from pore space at the rate that overburden is added (Hart et al., 1995). Effective stress remains approximately constant with increasing burial depth. Additional increments of overburden stress during burial are completely carried by the pore fluid, causing R to increase. Eventually diagenetic cement replaces overpressured pore fluid as the primary buttress against further consolidation. At this point, the black shale becomes fully elastic, with S_h coupling to P_p (e.g., Engelder and Fischer, 1994; Yassir and Bell, 1994; Hillis, 2001; Goulty, 2003). This poroelastic behavior is expressed by the following expression:

$$S_h = \frac{\nu}{1-\nu}(S_v - \alpha P_p) + \alpha P_p \qquad (7)$$

where α is the Biot poroelastic coefficient, and ν is Poisson's ratio (Anderson et al., 1973). As long as overburden remains constant, P_p-driven changes in S_h in lithified rock are governed by elastic properties and follow a stress path, κ, in S_h-versus-P_p space given by

$$\kappa = \frac{\Delta S_h}{\Delta P_p} = \alpha \frac{1-2\nu}{1-\nu} \qquad (8)$$

(e.g., Santarelli et al., 1998; Hillis, 2001; Goulty, 2003). Depending on in-situ poroelastic properties of a rock, κ can range from 0.4 to 0.88 (Santarelli et al., 1998). This behavior differs from unlithified sediment, where a change in P_p drives an equal change in S_h.

Presumably, the Dunkirk Shale entered the oil window after cementation rendered the rock fully elastic. At this time, flattened organic particles in low-permeability finely laminated black shale clay layers began to convert to bitumen. Assuming that kerogen was pervasive in pore space, the resultant increase in P_p resulted in a poroelastic response according to equation 8. The stress path, κ, followed by the black shale as it became overpressured can be illustrated by plotting R against λ, the ratio of pore pressure to overburden pressure stress, both normalized to S_v (Figure 11). Increasing P_p will induce cracks in the lithified clay matrix around kerogen flakes, the orientation of crack propagation being dependent on the extent to which S_h was modified by poroelastic deformation. Vertical microcracks are favored when κ follows a slope low enough to intersect the P_p trend line ($S_h = P_p$) where $R < 1$ ($S_h < S_v$). Horizontal microcracks are favored if κ follows a slope so steep that it intersects the $\lambda = 1$ line ($S_v = P_p$) where $R > 1$ ($S_v < S_h$). Steep stress paths, which describe a rapid modification of S_h by poroelastic deformation, are promoted by relatively low ν and high α values (Figure 11).

Drained consolidation of organic-rich silty clay yields a higher R than that resulting from the drained consolidation of sand as per equation 6 (Figure 12).

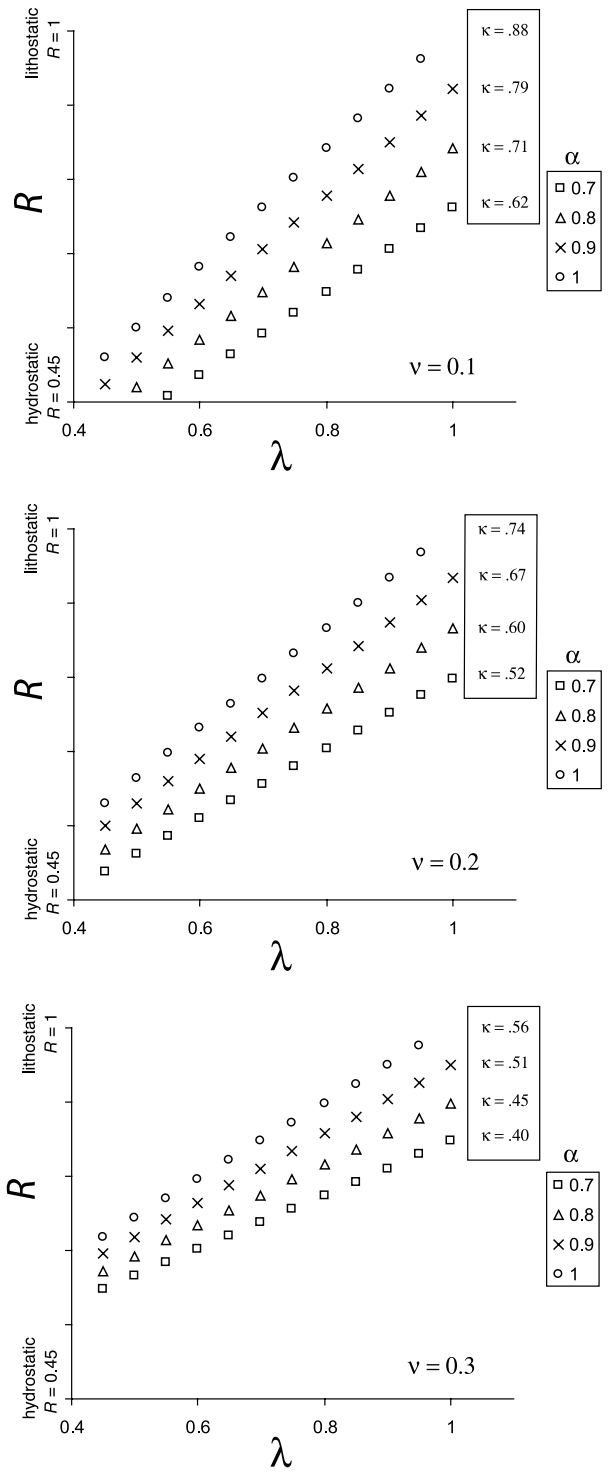

Figure 11. Examples of stress paths, κ, plotted as stress ratio, *R*, versus λ for conditions at 2-km (1.2-mi) burial depth, assuming ρ_{ob} = 2.3 g/cm^3. The purpose of these diagrams is to illustrate how various combinations of ν and α affect κ. Note that the values for *R* at λ = 0.45 do not necessarily represent in-situ conditions because they are calculated using equations 6 and 7 and the given poroelastic properties, ν and α.

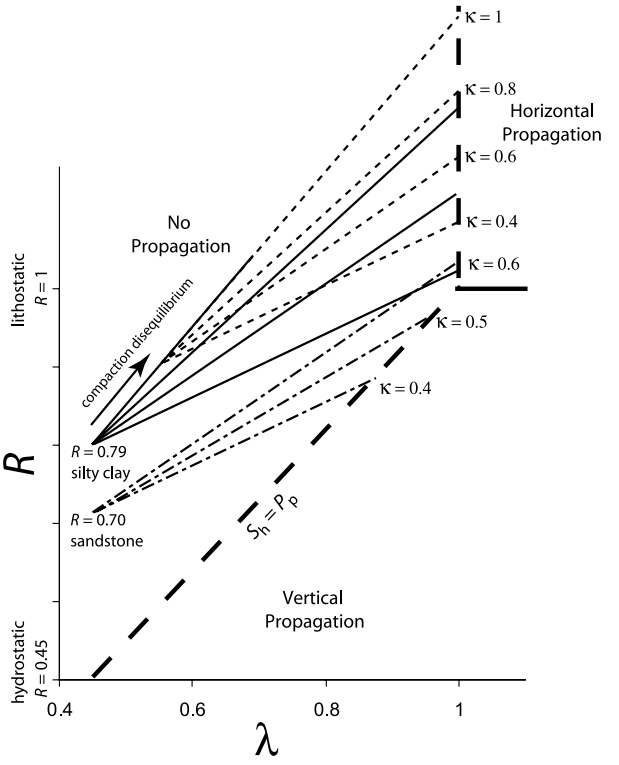

Figure 12. Stress paths, κ, for various elastic properties of black shale and sandstone plotted as a stress ratio, *R*, versus λ. Note that values for *R* at λ = 0.45 represent drained conditions at the time of lithification of black shale. The starting position of the potential stress paths of silty clay affected by compaction disequillibrium prior to maturation reflects elevated *R* and λ resulting from increased P_P as discussed in the text.

Following cementation, poroelastic deformation of a sandstone following κ < 0.6 ultimately results in the propagation of vertical microcracks (Figure 12). Such behavior may account for the great abundance of vertical joints in sandier beds of the Catskill delta complex (e.g., McConaughy and Engelder, 2001; Lash et al., 2004). Thermal maturation and related poroelastic deformation of silty clay deposits favor horizontal microcrack propagation over a larger range of elastic properties and consequent values of κ (Figure 12). Moreover, the deformation of these deposits when compaction disequilibrium (i.e., greater than hydrostatic initial values of *R* and λ) precedes maturation, as was the case for the black shale of the Catskill delta complex (e.g., Engelder and Oertel, 1985), increases the likelihood of horizontal microcracking (Figure 12). On a larger scale, however, the integrated elastic properties of sections more than a few meters thick are such that κ is relatively low, thus favoring vertical joint propagation.

In sum, the initiation of horizontal microcracking of the finely laminated, organic-rich deposits of the lower part of the Dunkirk Shale induced by catagenesis is favored by three material properties of these rocks: (1) abundant flat kerogen grains oriented parallel to layering; (2) a marked layer-perpendicular strength anisotropy in large part caused by the laminated nature of the rock; and (3) the tight, strongly oriented planar clay-grain fabric capable of sustaining P_p generated by the conversion of kerogen to bitumen and oil. The level of internal pressure necessary to initiate horizontal open-mode microcracks is a function of the first factor. That is, the flatter the kerogen particle, the lower the P_p necessary to create an effective tensile stress in the vertical direction. However, even if the requisite P_p is produced during catagenesis, it cannot be allowed to drain off. Indeed, the moderately bioturbated, relatively porous shale that dominates the upper half of the Dunkirk Shale likely remained drained during catagenesis, thereby precluding the initiation of horizontal microcracks. The tight microfabric of the laminated shale, inherited from its depositional and early diagenetic history, sustained P_p, the crack-driving stress, around pervasive kerogen particles converting to bitumen, favoring the initiation of horizontal microcracks, especially from the flattest kerogen grains. The level of P_p loss caused by microcracking appears to have been less than that generated by the conversion of kerogen to bitumen, thereby enabling the rock to pressurize. Internal pressure may have been further sustained by the filling of fractures by bitumen (e.g., Anissimov, 2001).

Following initiation, the orientation of crack propagation is controlled largely by in-situ stress. Overpressure development and resultant poroelastic deformation of the low-permeablility, finely laminated black shale deposits lower in the Dunkirk Shale reoriented the in-situ stress to a configuration in which $S_v < S_h$, thereby encouraging the widespread propagation of horizontal microcracks. Our calculations suggest that the local crack-driving stress induced by the poroelastic behavior of the organic-rich Dunkirk Shale alone could have initiated the observed horizontal microcracks. Still, preferential microcracking of the finely laminated shale suggests that material properties, including strength anisotropy and kerogen particle shape, were instrumental in initiating the horizontal cracks in these rocks. Poroelastic behavior and related switching of the in-situ stress field likely was enhanced by compaction disequilibrium. Indeed, a review of equation 3 indicates that an increase of R arising from compaction disequilibrium and consequent poroelastic coupling of S_h to P_p would have reduced the ΔP_p increment produced by catagenesis necessary to initiate horizontal microcracks.

CONCLUSIONS

Horizontal microcracks, most filled with bitumen, are exclusive to clay layers in the finely laminated, organic carbon-rich lower half of the Dunkirk Shale. The clay layers are defined by a tight, strongly oriented, platy grain microfabric produced by gravitational compaction early in the diagenetic history of these deposits. Note that moderately bioturbated, less organic-rich shales higher in the Dunkirk, defined by a more open or random microfabric, lack horizontal microcracks. Horizontal microcracking under a basinal stress field in which the greatest principal stress was vertical can be explained by (1) a marked compaction-induced layer-perpendicular strength anisotropy and abundant flattened kerogen grains, both vital to the initiation of microcracks in laminated shale in the lower half of the Dunkirk Shale and (2) poroelastic deformation of these low-permeability deposits pressurized by the conversion of kerogen to bitumen and the consequent establishment of a local in-situ stress field favorable to the propagation of the microcracks in the horizontal plane.

Natural fractures increase the effective permeability of otherwise tight source rocks. Horizontal microcracks produced early in the catagenic history of a source rock, like those documented in this article, would enhance lateral primary migration of hydrocarbons, especially in the updip direction, and may connect with vertical joints and/or faults, further facilitating primary and secondary migration. Horizontal microcracking of impermeable organic-rich horizons in shale-dominated basinal sequences would enhance fluid movement through these deposits; immediately over- and underlying unfractured intervals, however, may serve as aquitards, thereby maintaining elevated formation pressures in the fractured rocks.

REFERENCES CITED

Anderson, R. A., D. S. Ingram, and A. M. Zanier, 1973, Determining fracture pressure gradients from well logs: Journal of Petroleum Technology, v. 26, p. 1259–1268.

Anissimov, L., 2001, Overpressure phenomena in the Precaspian basin: Petroleum Geoscience, v. 7, p. 389–394.

Breckels, I. M., and H. A. van Eekelen, 1982, Relationship between horizontal stress and depth in sedimentary basins: Journal of Petroleum Technology, v. 34, p. 2191–2198.

Capuano, R. M., 1993, Evidence of fluid flow in microcracks in geopressured shales: AAPG Bulletin, v. 77, p. 1303–1314.

Comer, J. B., and H. H. Hinch, 1987, Recognizing and quantifying expulsion of oil from the Woodford Formation and age-equivalent rocks in Oklahoma and Arkansas: AAPG Bulletin, v. 71, p. 844–858.

Costin, L. S., 1981, Static and dynamic behaviour of oil shale, *in* S. W. Freiman, ed., Fracture mechanics of ceramics, rocks and concrete: American Society of Testing Materials, Philadelphia, ASTM STP 745, p. 169–184.

Demaison, G. J., and G. T. Moore, 1980, Anoxic environments and oil source bed genesis: AAPG Bulletin, v. 64, p. 1179–1209.

Dewhurst, D. N., A. C. Aplin, J.-P. Sarda, and Y. Yang, 1998, Compaction-driven evolution of porosity and permeability in natural mudstones: An experimental study: Journal of Geophysical Research, v. 103, p. 651–661.

du Rouchet, J., 1981, Stress fields, a key to oil migration: AAPG Bulletin, v. 65, p. 445–459.

Engelder, T., and M. P. Fischer, 1994, Influence of poroelastic behavior on the magnitude of minimum horizontal stress, S_h, in overpressured parts of sedimentary basins: Geology, v. 22, p. 949–952.

Engelder, T., and G. Oertel, 1985, The correlation between undercompaction and tectonic jointing within the Devonian Catskill delta: Geology, v. 13, p. 863–866.

Ervine, W. R., and J. S. Bell, 1987, Subsurface in situ stress magnitudes from oil-well drilling records: An example from the Venture area, offshore eastern Canada: Canadian Journal of Earth Science, v. 24, p. 1748–1759.

Espitalie, J., 1986, Use of T_{max} as a maturation index for different types of organic matter. Comparison with vitrinite reflectance, *in* J. Burrus, ed., Thermal modeling in sedimentary basins: Paris, Editions Technip, p. 475–496.

Finkbeiner, R. and M. D. Zoback, 1998, In-situ stress and pore pressure in the south Eugene Island field, Gulf of Mexico: Society Petroleum Engineers–International Society for Rock Mechanics Eurock 98 Conference, Trondheim, Norway, July 8–10, SPE Paper 47212, v. 1, p. 69–78.

Flügel, E., 1982, Microfacies analysis of limestones: Berlin, Springer-Verlag, 633 p.

Gaarenstroom, L., R. A. J. Tromp, M. C. de Jong, and A. M. Brandenburg, 1993, Overpressures in the central North Sea: Implications for trap integrity and drilling safety, *in* J. R. Parker, ed., Petroleum geology of northwestern Europe: Proceedings of the 4th Conference, Geological Society (London), p. 1305–1313.

Goulty, N. R., 2003, Reservoir stress path during depletion of Norwegian chalk oilfields: Petroleum Geoscience, v. 9, p. 233–241.

Grauls, D. J., and J. M. Baleix, 1994, Role of overpressures and in situ stresses in fault-controlled hydrocarbon migration: A case study: Marine and Petroleum Geology, v. 11, p. 734–742.

Harrold, T. W. D., R. E. Swarbrick, and N. R. Goulty, 1999, Pore pressure estimation from mudrock porosities in Tertiary basins, southeast Asia: AAPG Bulletin, v. 83, p. 1057–1067.

Hart, B. S., P. B. Flemings, and A. Deshpande, 1995, Porosity and pressure: Role of compaction disequilibrium in the development of geopressures in a Gulf Coast Pleistocene basin: Geology, v. 23, p. 45–48.

Hillis, R. R., 2001, Coupled changes in pore pressure and stress in oil fields and sedimentary basins: Petroleum Geoscience, v. 7, p. 419–425.

Jarvie, D. M., and L. L. Lundell, 2001, Kerogen type and thermal transformation of organic matter in the Miocene Monterey Formation, *in* C. M. Isaacs and J. Rulkötter, eds., The Monterey Formation: From rocks to molecules: New York, Columbia University Press, p. 268–295.

Karig, D. E., and G. Hou, 1992, High-stress consolidation experiments and their geological implications: Journal of Geophysical Research, v. 97, p. 289–300.

Karig, D. E., and J. Morgan, 1994, Tectonic deformation: Stress paths and strain history, *in* A. Maltman, ed., The geological deformation of sediments: London, Chapman & Hall, p. 167–204.

Katsube, T. J., and M. A. Williamson, 1998, Shale petrophysical characteristics: Permeability history of subsiding shales, *in* J. Scheiber, W. Zimmerle, and P. Sethi, eds., Shales and mudstones, I: Stuttgart, E. Schwiezerbart'sche, p. 69–91.

Kattai, V., 1994, Nature of the solid bitumen lenses in the lower Palaeozoic sedimentary rocks in northern Estonia: Oil Shale, v. 11, p. 100.

Krushin, J. T., 1997, Seal capacity of non-smectite shale, *in* R. C. Surdam, ed., Seals, traps, and the petroleum system: AAPG Memoir 67, p. 31–67.

Lambe, T. W., and R. V. Whitman, 1969, Soil mechanics: New York, John Wiley, 553 p.

Langford, F. F., and M.-M. Blanc-Valleron, 1990, Interpreting Rock-Eval pyrolysis data using graphs of pyrolizable hydrocarbons vs. total organic carbon: AAPG Bulletin, v. 74, p. 799–804.

Lash, G. G., and D. R. Blood, 2004, Origin of shale fabric by mechanical compaction of flocculated clay: Evidence from the Upper Devonian Rhinestreet Shale, western New York: Journal of Sedimentary Research, v. 74, p. 110–116.

Lash, G. G., S. Loewy, and T. Engelder, 2004, Preferential jointing of Upper Devonian black shale, Appalachian plateau, U.S.A.: Evidence supporting hydrocarbon generation as a joint-driving mechanism, *in* J. Cosgrove and T. Engelder, eds., The initiation, propagation, and arrest of joints and other fractures: Geological Society (London) Special Publication 231, p. 129–151.

Lawn, B., 1993, Fracture of brittle solids, 2d ed.: Cambridge, Cambridge University Press, 378 p.

Lehner, F. K., 1991, Pore-pressure induced fracturing of petroleum source rocks. Implications for primary migration, *in* G. Imarisio, M. Frias, and J. M. Bemtgen, eds., The European Oil and Gas Conference, a multidisciplinary approach in exploration and production R&D proceedings: London, Graham and Trotman, p. 142–154.

Lewan, M. D., 1987, Petrographic study of primary petroleum migration in the Woodford Shale and related rocks, *in* B. Doligez, ed., Migration of hydrocarbons in sedimentary basins: Paris, Editions Technip, p. 113–130.

Lewan, M. D., M. E. Henry, D. K. Higley, and J. K. Pitman, 2002, Material-balance assessment of the New Albany–Chesterian petroleum system of the Illinois basin: AAPG Bulletin, v. 86, p. 745–778.

Littke, R., D. R. Baker, and D. Leythaeuser, 1988, Microscopic and sedimentologic evidence for the generation and migration of hydrocarbons in Toarcian source rocks of different maturities: Organic Geochemistry, v. 13, p. 549–559.

Lomando, A. J., 1992, The influence of solid reservoir bitumen on reservoir quality: AAPG Bulletin, v. 76, p. 1137–1152.

Márquez, X. M., and E. W. Mountjoy, 1996, Microcracks due to overpressures caused by thermal cracking in well-sealed Upper Devonian reservoirs, deep Alberta basin: AAPG Bulletin, v. 80, p. 570–588.

McConaughy, D. T., and T. Engelder, 2001, Joint initiation in bedded clastic rocks: Journal of Structural Geology, v. 23, p. 203–221.

Meissner, F. F., 1978, Petroleum geology of the Bakken Formation,

Williston basin, North Dakota and Montana: Williston Basin Symposium, Montana Geological Society, 24th Annual Conference, p. 207–227.

Momper, J. A., 1978, Oil migration limitations suggested by geological and geochemical considerations, *in* W. H. Roberts and R. Cordell, eds., Chemical constraints on petroleum migration: AAPG Continuing Short Course Notes Series 8, B1–B60.

O'Brien, N. R., and R. M. Slatt, 1990, Argillaceous rock atlas: New York, Springer-Verlag, 141 p.

Özkaya, I., 1988, A simple analysis of oil-induced fracturing in sedimentary rocks: Marine and Petroleum Geology, v. 5, p. 293–297.

Pitman, J. K., L. C. Price, and J. A. LeFever, 2001, Diagenesis and fracture development in the Bakken Formation, Williston basin: Implications for reservoir quality in the middle member: U.S. Geological Survey Professional Paper 1653, 19 p.

Santarelli, R. J., J. T. Tronvoll, M. Svennekjaer, H. Skele, R. Henriksen, and R. K. Bratli, 1998, Reservoir stress path: The depletion and the rebound: Society Petroleum Engineers–International Society for Rock Mechanics Eurock 98 Conference, Trondheim, Norway, July 8–10, SPE Paper 47350, v. 2, p. 203–209.

Schmidt, R. A., 1977, Fracture mechanics of oil shale-unconfined fracture toughness, stress corrosion cracking, and tension test results, *in* F.-D. Wang and G. B. Clark, eds., Energy resources and excavation technology: Proceedings, 18th U.S. Symposium on Rock Mechanics: Golden, Colorado, Colorado School of Mines, p. 2A2-1–2A2-6.

Snarsky, A. N., 1962, Die primare migration des erdols: Freiberger Forschungsch, v. C123, p. 63–73.

Swarbrick, R. E., M. J. Osborne, and G. S. Yardley, 2002, Comparison of overpressure magnitude resulting from the main generating mechanisms, *in* A. R. Huffman and G. L. Bowers, eds., Pressure regimes in sedimentary basins and their prediction: AAPG Memoir 76, p. 1–12.

Talukdar, S., O. Gallango, C. Vallejos, and A. Ruggiero, 1987, Observations on the primary migration of oil in the La Luna source rocks of the Maracaibo Basin, Venezuela, *in* B. Doligez, ed., Migration of hydrocarbons in sedimentary basins: Paris, Editions Technip, p. 59–78.

Tissot, B., and D. H. Welte, 1984, Petroleum formation and occurrence: New York, Springer-Verlag, 699 p.

Vernik, L., 1994, Hydrocarbon-generation–induced microcracking of source rocks: Geophysics, v. 59, p. 555–563.

Yassir, N. A., and J. S. Bell, 1994, Relationships between pore pressure, stresses, and present-day geodynamics in the Scotian Shelf, offshore eastern Canada: AAPG Bulletin, v. 78, p. 1863–1880.